Direct observation of the electron spectral function in the integer and fractional quantum Hall regimes by resonant tunneling

G. S. Boebinger, A. F. J. Levi, A. Passner, L. N. Pfeiffer, and K. W. West
AT&T Bell Laboratories, Murray Hill, New Jersey 07974
(Received 9 November 1992)

Low-temperature current-voltage characteristics of a double-barrier resonant tunnel junction are used to directly measure the two-dimensional (2D) electron spectral function. Our data provide quantitative determination of the 2D density of states, including chemical potential and linewidth oscillations as a function of magnetic field up to 51 T. We also measure a chemical potential jump at $\frac{1}{3}$ fractional filling of the lowest Landau level.

It is often possible to describe the net current I flowing from electrode 1 and electrode 2 via a tunnel barrier by[1]

$$I=2e\frac{2\pi}{\hbar}\sum_{\mathbf{k}_1\mathbf{k}_2}|M_{\mathbf{k}_1\mathbf{k}_2}|^2\int d\varepsilon[f(\varepsilon)-f(\varepsilon+\Delta\varepsilon)]\times A_1(\mathbf{k}_1,\varepsilon)A_2(\mathbf{k}_2,\varepsilon+\Delta\varepsilon)\,, \tag{1}$$

where $\Delta\varepsilon$ is the potential drop across the barrier and e is the electron charge. This expression sums between initial states with wave vector $\mathbf{k}_1$, energy ε, and final states $\mathbf{k}_2$, $\varepsilon+\Delta\varepsilon$, separated by the tunnel barrier. The matrix element $|M_{\mathbf{k}_1\mathbf{k}_2}|^2$ is the coupling strength between initial and final k states and $f(\varepsilon)$ is the Fermi function, assuming the occupation of initial and final states are separately in thermal equilibrium. The density of states enters through the spectral function $A(\mathbf{k},\varepsilon)$. For the special case of noninteracting electrons of energy E one finds $A(\mathbf{k},\varepsilon)=\delta(E-\hbar^2\mathbf{k}^2/2m^*)$ where m^* is the effective electron mass. However, in the more general case of interacting electrons, $A(\mathbf{k},\varepsilon)=1/\pi\,\mathrm{Im}G$ where G is the Green's function for interacting electrons in the initial or final state.

Equation (1) is, in essence, the transfer Hamiltonian method of Bardeen[2] in which it is assumed that tunneling probability is small and it is possible to treat initial and final states as independent separable quantities. A surprisingly large number of single-barrier tunneling experiments have been successfully described using this model.[1] The theoretical justification for such an apparently successful approach has been discussed,[3] and few experimental results have challenged the theory.[4] Hence, tunneling can be a reliable means by which to measure the single-particle electron spectral function.[5]

It is also possible to describe the current-voltage (I_C-V_{CE}) characteristics of a double-barrier resonant tunnel junction using Eq. (1).[6,7] Our earlier work[7] considered only the high magnetic-field limit in which all electrons occupy the lowest Landau level in the emitter. In that work, a single energy level in the spectral function of the two-dimensional (2D) emitter was used to study the spectral function of the quantum well. An alternative, which we describe here, is to use the empty states of the quantum well to probe the self-energy of electrons in the 2D emitter in the integral and fractional quantum Hall regimes.

Our double-barrier resonant tunnel structures (see inset. Fig. 1) are grown on ⟨100⟩-oriented undoped semi-insulating GaAs substrates at 610 °C using molecular-beam epitaxy. A 5000-Å n-type (2×10^{18} cm^{-3} Si impurities) GaAs emitter contact layer is deposited on the substrate. This is followed by a 700-Å GaAs setback layer, grown to ensure minimal diffusion of Si impurities into the double-barrier structure. The first AlAs tunnel barrier is 48-Å thick, the GaAs well is 99-Å thick, and the second AlAs barrier is 31-Å thick. Crystal growth is completed by depositing a 200-Å GaAs setback layer followed by a 3000-Å n-type (2×10^{18} cm^{-3} Si impurities) GaAs collector contact layer. This structure is designed so that electrons tunnel from a high-mobility 2D accumulation layer through a wide AlAs barrier into a nominally empty 2D GaAs quantum well. Later, we will show that the 2D electron density in the emitter ρ is accurately given by $\rho=(14.7V_{CE}+0.5)\times10^{11}$ cm^{-2} over the entire range of 0.1 V$\le V_{CE}\le$0.4 V. After removal from the growth chamber the wafers are etched into approximately 90-μm-diameter mesas and separate Ohmic contacts are made to the emitter and collector.

The current-voltage characteristics of resonant tunnel junctions are measured at low temperatures ($T<4.2$ K) in fixed magnetic fields applied parallel to the direction of current flow through the tunnel structure. For $B\le15$ T the measurements are made in a superconducting magnet. For magnetic fields up to $B=51$ T, the measurements are made in a quasistatic magnetic field (constant within $\pm0.2\%$) during ~0.5 ms at the peak of a sinusoidal magnetic-field pulse. As the voltage bias is applied across the sample, the tunnel current is measured by a current-sensitive amplifier located outside the magnetic field. Care is taken to minimize series resistances which can limit the ability to accurately measure currents in regions of large negative differential conductivity.

In Fig. 1, the solid line gives the logarithm of collector current I_C as a function of applied collector-emitter voltage bias V_{CE} for (a) $B=0$ T and (b) $B=15$ T. In Fig. 1 only we have subtracted a small nonresonant background current of $0.04\exp(V_{CE}/0.128\ \mathrm{V})$ μA. The inset in the figure shows the conduction-band profile for the device under bias, where $\Delta\varepsilon$ is the energy difference between initial and final states. The large peak in current at

$V_{CE}=0.118$ V is due to elastic tunneling ($\Delta\varepsilon\equiv 0$ meV) from the degenerate 2D electron system in the emitter to the unoccupied lowest-energy 2D subband of the 99-Å quantum well. The full width at half maximum (FWHM) of this peak is only 2.9 meV, much less than the emitter Fermi energy (7.9 meV) at $V_{CE}=0.118$ V. This is clear evidence that tunneling originates from a 2D emitter. No hysteresis in the I_C-V_{CE} characteristic is detected, indicating no appreciable electron space charge in the quantum well (since the second AlAs barrier is much thinner than the first). As a result, to a very good approximation, the applied voltage V_{CE} is proportional to $\Delta\varepsilon$. The accuracy of this proportionality is verified for $0.1\le V_{CE}\le 0.5$ V and $0\le B\le 51$ T using known cyclotron and LO-phonon excitation energies in the device.[7–9] We find $\Delta\varepsilon(\text{eV})=0.37[V_{CE}-0.118\text{ V}]$ which is excellent quantitative agreement with the solution of Poisson's equation in our device.

We note that the $B=0$ T elastic resonance line shape is asymmetric and cannot be described by either a Lorentzian or Gaussian [dotted and dashed lines in Fig. 1(a)]. Either elastic[10] or inelastic tunneling processes may result in such a high-energy tail. The low-energy side of the resonance exhibits the sharper cutoff due to the absence of available final states in the quantum well.

At sufficiently large bias voltages it is possible for a tunneling electron to emit a GaAs longitudinal-optic (LO) phonon of energy $\hbar\omega_{GaAs}=36.4$ meV in the GaAs quantum well or an AlAs LO phonon of energy $\hbar\omega_{AlAs}=50.2$ meV in the AlAs barrier.[11] These phonon processes give rise to two inelastic peaks[7–9] at $V_{CE}=0.210$ and 0.255 V which are significantly broader than the elastic resonance peak, due to smearing by the emitter Fermi energy (12 and 14 meV at $V_{CE}=0.210$ and 0.255 V, respectively). A best fit to the Gaussian line shapes (dashed curves in Fig. 1) yields FWHM (GaAs)=17 meV and FWHM (AlAs)=21 meV.

The data change greatly when a magnetic field is applied parallel to the direction of current flow through the device. Figure 1(b) shows the $\log_{10}(I_C)-V_{CE}$ trace for

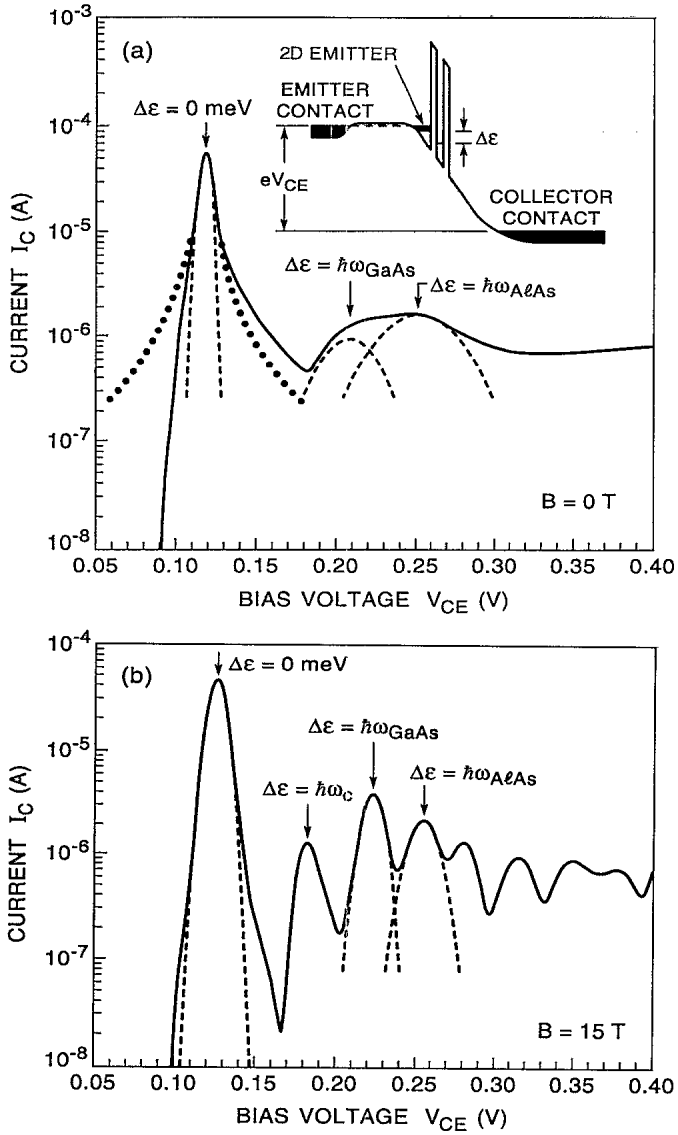

FIG. 1. (a) Measured resonant tunneling current I_C as a function of applied voltage V_{CE} at $T=1.0$ K and $B=0$ T. A small nonresonant background current has been subtracted, as described in the text. The elastic resonance peak is at $V_{CE}=0.118$ V. The line shape is neither Gaussian (dashed curve) nor Lorentzian (dotted curve). Peaks associated with GaAs and AlAs single LO-phonon emission occur at bias $V_{CE}=0.210$ and 0.255 V, respectively. The inset shows a schematic conduction-band diagram for the device under bias. (b) Same as (a) but for $B=15$ T applied parallel to the direction of current flow. Dashed curves are Gaussians fit to the elastic resonance and single LO-phonon emission resonances.

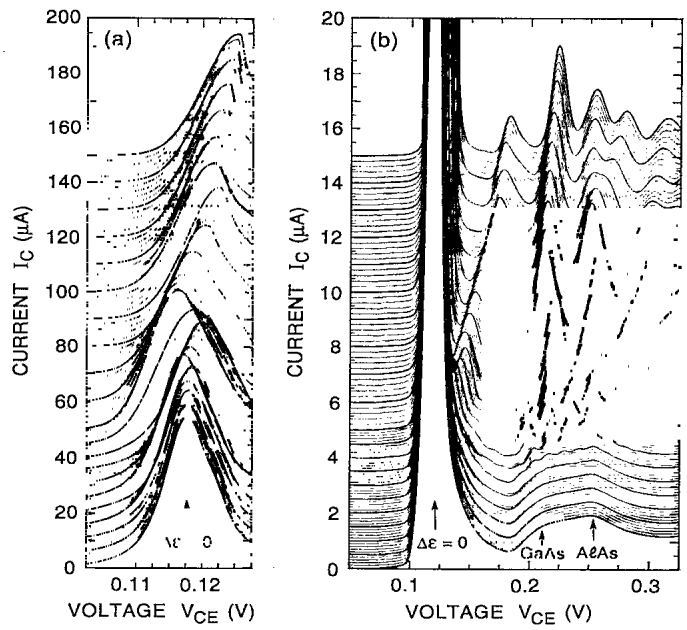

FIG. 2. (a) I_C-V_{CE} traces of the elastic resonance for $T=1.0$ K and $0\le B\le 15$ T. The lowest trace corresponds to $B=0$ T and the uppermost corresponds to $B=15$ T. The traces are offset for clarity by 10 μA/T. Note the sudden shifts in peak position to lower bias which are periodic in inverse magnetic field. (b) Entire I_C-V_{CE} traces on an amplified vertical scale showing resonances associated with LO-phonon emission and inter-Landau-level tunneling. Peak position shifts similar to those for the elastic resonance in Fig. 2(a) are observed.

$B=15$ T. Additional resonances are observed[9,12–14] because 2D electron states in the emitter and the quantum well are further quantized into Landau levels of index $n=0,1,2,\ldots,$ separated by the cyclotron energy $\omega_c=eB/m^*c$. Hence, for noninteracting electrons, we expect narrow resonances at $\Delta\varepsilon=0$, $\hbar\omega_{\mathrm{GaAs}}+n\hbar\omega_c$, and $\hbar\omega_{\mathrm{AlAs}}+n\hbar\omega_c$. Resonances at $\Delta\varepsilon=n\hbar\omega_c$ exist only in the presence of elastic angular-momentum-breaking tunneling processes.

Most notably, the elastic peak at $B=15$ T no longer exhibits the pronounced asymmetry observed at $B=0$ T. Its line shape is well described by a Gaussian with a FWHM of 4.6 meV, which is a 60% *increase* in linewidth compared to the $B=0$ value. Even more dramatic changes occur in the GaAs and AlAs LO-phonon lines, for which Landau-level quantization at $B=15$ T *decreases* the linewidths by nearly a factor of 3, to FWHM(GaAs)=5.4 meV and FWHM(AlAs)=7.6 meV. It is not clear why the integrated peak area of the GaAs LO-phonon line is relatively unchanged by a magnetic field, while the integrated peak area of the AlAs LO-phonon line decreases by almost a factor of 2.

Figure 2(a) contains the portion of the I_C-V_{CE} traces for $0\le B\le 15$ T which show the elastic tunneling resonance. The bottom trace is for $B=0$ T and the uppermost trace is for $B=15$ T. Each trace is offset vertically by 10 μA/T. Note that the peak position oscillates with magnetic field.[15] These oscillations are periodic in $1/B$ and arise from magnetic-field-induced depopulation of Landau levels in the 2D emitter. Upon depopulation, the chemical potential in the 2D emitter jumps rapidly and the chemical potentials of the 3D emitter contact and the 2D emitter reequilibrate. This lowers V_{CE} bias at the elastic tunneling resonance. The $1/B$ periodicity directly yields the 2D electron density, $\rho=2.2\times10^{11}$ cm^{-2}, and the Fermi energy, $E_F=7.9$ meV, at a bias of $V_{\mathrm{CE}}=0.118$ V.

Complete I_C-V_{CE} traces for $0\le B\le 15$ T are shown in Fig. 2(b) on an expanded vertical scale. The elastic resonance and two LO-phonon resonances are labeled. Additional resonances result from the inter-Landau-level tunneling processes which give rise to Landau levels fanning out from each of the three $B=0$ T resonances.[9,12–14] As can be seen, many resonances display peak position shifts due to magnetic depopulation in the

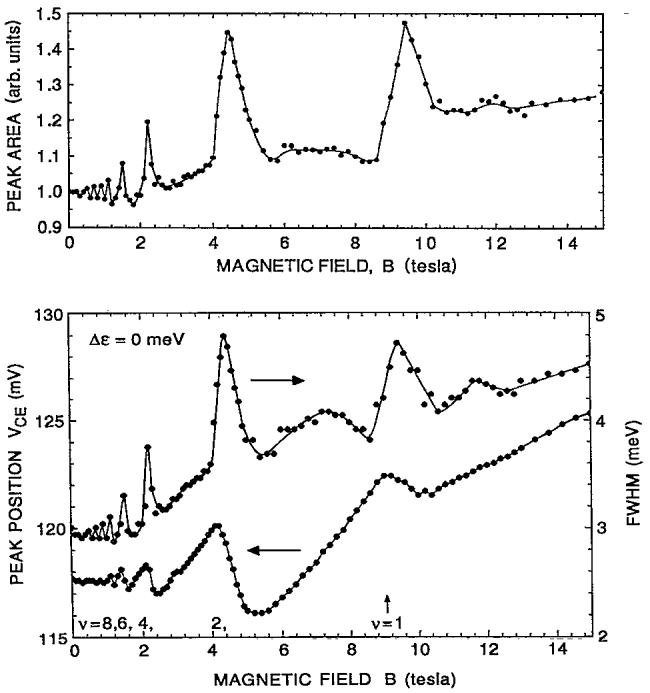

FIG. 3. Measured elastic resonance peak position and FWHM as a function of magnetic field B. The upper panel contains the integrated peak area, normalized to the $B=0$ T value. The shifts in peak positon accompanied by upward cusps in the FWHM and peak area correspond to chemical potential jumps in the 2D emitter concurrent with Landau-level line broadening at integer Landau-level filling factors.

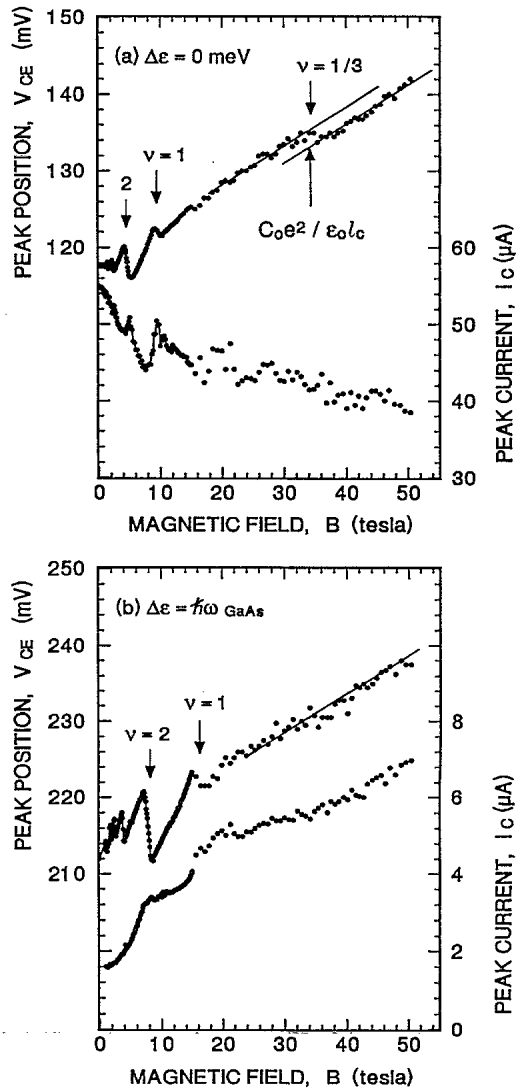

FIG. 4. Measured peak position and peak current for magnetic fields to $B=51$ T for (a) the elastic resonance and (b) the GaAs LO-phonon emission resonance. Note the chemical potential jump in the 2D emitter at $\frac{1}{3}$ fractional filling of the lowest Landau level. The measured chemical potential jump corresponds to $C_0\sim0.16$ (determined by equating the slope of the three solid lines to $\hbar\omega_c/2$).

emitter. From these shifts, we derived the dependence of ρ on V_{CE} which was given earlier.

Figure 3 contains the magnetic-field dependence of the elastic resonance peak position and FWHM from the data of Fig. 2(a). The upper panel contains the integrated peak area normalized to the $B=0$ T value. The sharp decreases in peak position at $B=1.15$, 1.5, 2.3, and 4.6 T occur at the Landau-level filling factor $\nu=2\pi\rho\hbar/eB=8$, 6, 4, and 2, respectively. The line shift at $B=9.2$ T evidences the depopulation of the higher-energy spin state of the lowest Landau level at $\nu=1$. The peak position reflects the magnetic-field dependence of the chemical potential in the 2D emitter. The magnitude of the line shift is proportional to the energy gap at these filling factors. We will calibrate this energy scale from data taken at $B>20$ T.

In the case of noninteracting electrons, the emitter spectral function would consist of δ functions and depopulation of energy levels would occur abruptly with chemical potential jumps equal to the bare energy gaps at integer filling. Instead, the data show depopulation occurs over finite ranges of magnetic field. The data in the upper traces of Fig. 3 show that depopulation of emitter energy levels is accompanied by cusps in the FWHM and integrated area of the resonance. Although electron density inhomogeneities could contribute to the observed cusps in the FWHM, they cannot account for the observed variations in peak area. These features probably both result from a decrease in screening in the 2D emitter and consequent decrease in electron lifetime when the chemical potential is pinned by localized states.[16]

In Fig. 4 we extend the data on the elastic and GaAs LO-phonon resonances to magnetic fields of $B=51$ T. In both cases, the peak positions display chemical potential oscillations periodic in $1/B$ and each resonance shifts by ~ 0.5 mV/T at the highest experimental fields (solid lines in Fig. 4). Equating this dependence with $\hbar\omega_c/2$ affords an approximate calibration of the absolute energy scale for the 2D emitter. Using this calibration we note from Figs. 3 and 4 that the observed shifts in chemical potential upon the Landau-level depopulation are comparable to $\hbar\omega_c$.

We now draw attention to evidence of a shift in the chemical potential near $\frac{1}{3}$ fractional filling of the lowest Landau level [$\nu=\frac{1}{3}$ in Fig. 4(a)]. We estimate the shift at $\frac{1}{3}$ filling to be 4.2 meV. Describing the fractional quantum Hall effect energy in terms of the Coulomb energy scale, $C_0e^2/\varepsilon_0 l_c$, where $l_c=(\hbar c/eB)^{1/2}$ is the magnetic length and ε_0 is the static dielectric constant, we find that $C_0\sim 0.16$. This is in accord with theoretical estimates of the energy gap of the $\nu=\frac{1}{3}$ fractional quantum Hall state,[17] if three $e/3$-charged quasiparticles must tunnel together.

Finally, in high magnetic fields there are qualitative differences between the integrated peak areas of elastic and phonon emission resonances. While the elastic peak current *decreases* with increasing field, its FWHM increases as $(2.5+0.48B^{1/2})$ meV, thereby maintaining a constant integrated peak area (within $\sim 15\%$). In contrast, the GaAs peak current *increases* dramatically while its FWHM remains a constant ~ 5.4 meV for $B\gtrsim 12$ T. The net result is a greater than fourfold increase in integrated peak area for GaAs LO-phonon-assisted tunneling from $B=0$ to 51 T. This is qualitatively explained by the increased phase space available for LO-phonon emission, because the number of unoccupied final states in the lowest Landau-level increases linearly with magnetic field. Thus, more LO-phonon assisted tunneling processes become possible in high magnetic fields, while the probability of elastic tunneling remains fixed.

In conclusion, resonant electron tunneling can provide direct measurement of electron self-energy effects in the 2D electron system. In this paper we report measurements of the magnetic-field dependence of density of states, chemical potential, and level broadening in the spectral function of a 2D electron system. We also report what is, to our knowledge, the first spectroscopic measurement of the chemical potential jump at $\frac{1}{3}$ fractional filling of the lowest Landau level.

The authors would like to thank A. H. MacDonald and C. M. Varma for useful discussions and D. L. Windt for assistance with processing data.

[1]See, for example, E. L. Wolf, *Principles of Electron Tunneling Spectroscopy* (Oxford University Press, New York, 1989).

[2]J. Bardeen, Phys. Rev. Lett. **6**, 57 (1961).

[3]See, for example, T. E. Feuchtwang, in *Inelastic Electron Tunneling Spectroscopy,* edited by T. Wolfram, Springer Series in Solid-State Sciences Vol. 4 (Springer-Verlag, Berlin, 1978), p. 129.

[4]P. Guéret *et al.*, Solid State Commun. **68**, 977 (1988).

[5]In contrast, it has been noted that observations of cyclotron resonance in 2D systems are not directly related to the electron spectral function. This is due, in part, to the strong dependence of the cyclotron resonance line shape on the intricate interplay of disorder and electron-electron interactions (including strong differences between donor and acceptor impurities). For more discussions of these issues, see E. Zaremba, Phys. Rev. B **44**, 1379 (1991); Dimitro Antoniou and A. H. MacDonald, *ibid.* **46**, 15 225 (1992); J. Richter, H. Sigg, K. von Klitzing, and K. Ploog, *ibid.* **39**, 6268 (1989).

[6]M. C. Payne, J. Phys. C **19**, 1145 (1986).

[7]G. S. Boebinger *et al.*, Phys. Rev. Lett. **65**, 235 (1990).

[8]V. J. Goldman *et al.*, Phys. Rev. B **36**, 7635 (1987).

[9]C. H. Yang *et al.*, Phys. Rev. B **40**, 6272 (1989); J. G. Chen *et al.*, *ibid.* **43**, 4531 (1991).

[10]J. Leo and A. H. MacDonald, Phys. Rev. Lett. **64**, 817 (1990).

[11]*Landolt-Bornstein Tables,* edited by O. Madelung, H. Schulz, and H. Weiss, Landolt-Börnstein New Series, Group 17, Vol. III, Pt. a (Springer-Verlag, Berlin, 1982).

[12]E. E. Mendez *et al.*, Phys. Rev. B **33**, 2893 (1986).

[13]M. L. Leadbeater *et al.*, Phys. Rev. B **39**, 3438 (1989).

[14]J. Smoliner *et al.*, Phys. Rev. B **39**, 12 937 (1989).

[15]V. J. Goldman *et al.*, in *Resonant Tunneling in Semiconductors Physics and Applications,* edited by L. L. Chang, E. E. Mendez, and C. Tejedor (Plenum, New York, 1991), p. 431.

[16]S. Das Sarma and X. C. Xie, Phys. Rev. Lett. **61**, 738 (1988); X. C. Xie *et al.*, Phys. Rev. B **42**, 7132 (1990).

[17]T. Chakraborty and P. Pietiläinen, in *The Fractional Quantum Hall Effect,* Springer Series in Solid-State Sciences Vol. 85 (Springer-Verlag, Heidelberg, 1988).